AD-A096 777 COLORADO STATE UNIV FORT COLLINS F/G 20/12
DYNAMIC MODELING OF PHYSICALLY SMALL AND HIGH-FREQUENCY SEMICON--ETC(U)
MAR 81 D K FERRY DAAG29-78-G-0061
UNCLASSIFIED ARO-15435.9-EL NL

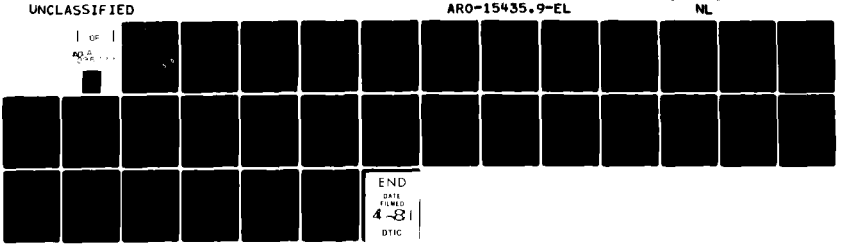

END
DATE FILMED
4-81
DTIC

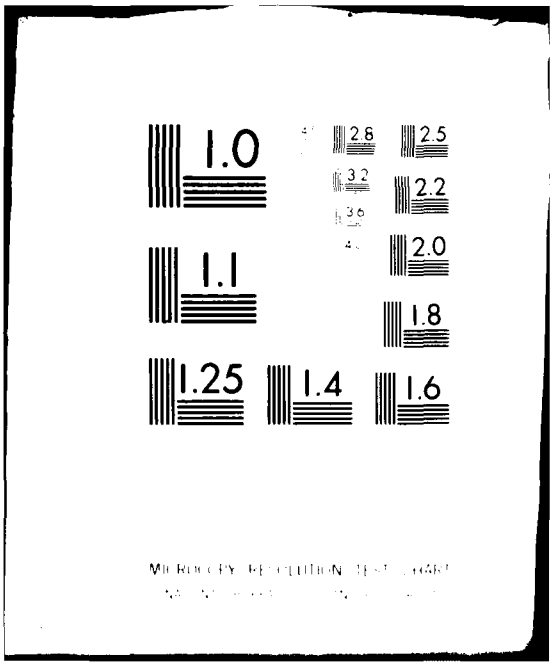
1.0
2.8
2.5
3.2
2.2
3.6
2.0
1.1
1.8
1.25
1.4
1.6

LEVEL II (12) 11

ARO 15435.9-EL

AD A096777

SECURITY CLASSIFICATION OF THIS PAGE (When Data Entered)

REPORT DOCUMENTATION PAGE

READ INSTRUCTIONS BEFORE COMPLETING FORM

1. REPORT NUMBER (6)	2. GOVT ACCESSION NO. AD-A096777
3. RECIPIENT'S CATALOG NUMBER	
4. TITLE (and Subtitle) Dynamic Modeling of Physically Small and High-Frequency Semiconductor Devices.	5. TYPE OF REPORT & PERIOD COVERED (9) Final Report.
6. PERFORMING ORG. REPORT NUMBER	
7. AUTHOR(s) (10) D. K. Ferry (15)	8. CONTRACT OR GRANT NUMBER(s) DAAG29-78-G-0061
9. PERFORMING ORGANIZATION NAME AND ADDRESS Colorado State University Fort Collins, Colorado 80523	10. PROGRAM ELEMENT, PROJECT, TASK AREA & WORK UNIT NUMBERS DRXRO-EL-15435
11. CONTROLLING OFFICE NAME AND ADDRESS Army Reserach Office Research Triangle Park, NC 27709	12. REPORT DATE (11) 1 March 1981
	13. NUMBER OF PAGES 30
14. MONITORING AGENCY NAME & ADDRESS (if different from Controlling Office) (12) 31	15. SECURITY CLASS. (of this report) (U)
	15a. DECLASSIFICATION/DOWNGRADING SCHEDULE

16. DISTRIBUTION STATEMENT (of this Report)

Distribution unlimited

DISTRIBUTION STATEMENT A
Approved for public release;
Distribution Unlimited

DTIC ELECTE MAR 24 1981 S D C

17. DISTRIBUTION STATEMENT (of the abstract entered in Block 20, if different from Report)

18. SUPPLEMENTARY NOTES
THE VIEW, OPINIONS, AND/OR FINDINGS CONTAINED IN THIS REPORT ARE THOSE OF THE AUTHOR(S) AND SHOULD NOT BE CONSTRUED AS AN OFFICIAL DEPARTMENT OF THE ARMY POSITION, POLICY, OR DECISION, UNLESS SO DESIGNATED BY OTHER DOCUMENTATION.

19. KEY WORDS (Continue on reverse side if necessary and identify by block number)

Semiconductor device, MESFET, transistor, ultra-small electronics

20. ABSTRACT (Continue on reverse side if necessary and identify by block number)

A program of research is reviewed that addressed transport in physically small (submicron-to-ultrasubmicron) and/or high frequency semiconductor devices. In devices of the 0.25 μm characteristic length, significant effects on the device performance arise from the fact that the carriers have characteristic response times on the order of the device transit time. Effects due to temporal (and spatial) memory retardation, finite-non-zero collision duration, intra-collisional field effects, and quantization within the device govern the transport. Additionally, device replication can lead to synergistic system performance.

DD FORM 1 JAN 73 1473 EDITION OF 1 NOV 65 IS OBSOLETE

(U) 088300

SECURITY CLASSIFICATION OF THIS PAGE (When Data Entered)

DTIC FILE COPY

81 3 23 048

This program of study has investigated the role these effects play through utilization of full two-dimensional device simulations that incorporate the various effects.

Dynamic Modeling of Physically Small and High Frequency Semiconductor Devices

FINAL REPORT

On

DAAG29-78-C-0061
DRXRO-EL-15435

1 March 1981

Dr. David K. Ferry
Professor and Head of Electrical Engineering
Colorado State University
Fort Collins, Colorado 80523

Abstract

A program of research is reviewed that addressed transport in physically small (submicron-to-ultrasubmicron) and/or high frequency semiconductor devices. In devices of the 0.25 μm characteristic length, significant effects on the device performance arise from the fact that the carriers have characteristic response times on the order of the device transit time. Effects due to temporal (and spatial) memory retardation, finite-non-zero collison duration, intra-collisional field effects, and quantization within the device govern the transport. Additionally, device replication can lead to synergistic system performance. This program of study has investigated the role these effects play through utilization of full two-dimensional device simulations that incorporate the various effects.

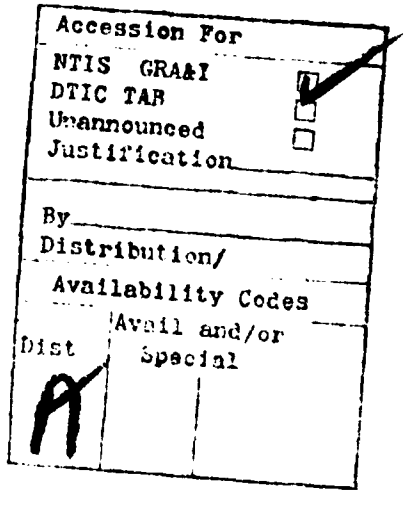

Table of Contents

I. Introduction

Over the last two decades, the growth of large-scale integration (LSI) has been phenomenal, and the application of special integrated circuits and microprocessors has blossomed. In fact, the complexity, as defined by the number of devices on an individual integrated circuit chip has approximately doubled each year over this time span [1]. There are, of course, several factors leading to this increase in complexity, including major effects arising from increased die size, increased circuit cleverness, and reduced device size. There are indications in recent times that this growth is slowing [2], and in fact Moore [1] suggested that this might arise as a consequence of a reduction in further increases in circuit design cleverness. It is not at all clear that this is the case, and it seems equally likely that the reduction in growth is due more to the fact that we are approaching some limitations on our fabrication technology and on our understanding of the physical limits of device performance in integrated systems. Certainly, the current trend of extrapolation of technology and design techniques can be expected to be subject to severe limitations as we enter the very-large-scale integration (VLSI) region, even though current design technology has certainly achieved relatively small devices in MOS [3-5], bipolar [6], and compound semiconductor [7] technology.

From the above discussion, it is apparent that one can reasonably ask just how far can we expect device size to be reduced, and do we understand the physical principles that will govern device behavior in that region of smallness. Previously, Hoeneisen and Mead [8,9] discussed minimal device size for MOS and bipolar devices based upon extrapolation and scaling of our present device structures. They considered a general study of the

static limitations imposed by oxide breakdown, source-drain punchthrough, ionization in the channel, etc., on typical MOS structures, and similar effects in the bipolars. Although they suggested a minimum channel length of 1100Å for the MOS, for example, it was found that a more typical device would have a channel length of 2500Å. Others have also approached this topic in a similar manner and have also considered the role of doping fluctuations, power dissipation, noise, and interconnections in limiting packing density of these devices [10]. And yet, for all of these studies, it is evident that the emphasis has been on other questions than whether or not our current understanding of device physics is pertinent to devices on that spatial scale [11]. Present day electron-beam lithography and photoresist technology is capable of addressing devices of that size, and in fact is apparently capable of producing linewidths (and device sizes) of 250Å [12]. With modifications of resist structures, even 80Å lines have been produced [13].

Even though Hoeneisen and Mead suggested that a size of 1100-2500Å channel length might be the minimum, current research endeavors have pushed to and even beyond these limits. Rockwell [14], has made MOSFETs of 0.25 μm channel length and width and operated them in a ring counter configuration. Texas Instruments has used selective etching to make MOSFETs of 0.1 μm channel length [15], and IBM has fabricated devices of a few hundred Angström channel length [16]. Similar progress is underway for MESFETs as well, where the critical length remains the gate length. Granted that technological momentum is pushing to ever smaller devices, and the technology is there to prepare really very small devices, it becomes obvious that we must now ask whether our physical understanding of devices and their operation can indeed by extrapolated

down to very small space (and time) scales, or do the underlying quantum electronic principles prevent a down-scaling of the essential semi-classical concepts upon which our current understanding is based? The purpose of the current work and the work proposed here is to address just this question.

In the following sections, we review the progress made under current ARO grant DRXRO-15435-EL, although part of this is deferred until Section III. The ARO program is primarily concerned with the physics of submicron devices.

II. Physics of Submicron Devices

In our research, we have attempted to lay a conceptual framework for an ultimate physics of small devices and the modeling necessary to characterize these devices. We borrow heavily from quantum theories of nonlinear electronic processes. Some of these have already been illustrated to be of importance, in hot-electron transport for example, but we recognize that the totality of such studies is small and not fully developed. Many of the effects will be far more significant in the lighter mass compound semiconductors [17] than in the silicon currently used. To approach this problem, we find it convenient to define two dimensional scales for small devices (where the dimension might be channel length for example): the medium-small device (MSD) with typical spatial extent of 2500Å, and the very-small device (VSD) with typical spatial extent of 250Å. The reader will note that these dimensions correlate with the typical small MOS device discussed by Hoeneisen and Mead [8] and with the small structures prepared by Broers, et al., [12]. MSD's

provide a scale upon which it is not unreasonable to expect that the physics will be well approximated by extrapolations from present day device physics but with certain new features anticipated from quantum physics which modify considerably the device performance. MSD's might therefore be similar in concept, but not necessarily in performance, to present day structures. However, on the VSD scale, a fully quantum mechanical understanding appears necessary, and indeed new device structures may well be possible which fully exploit the possibilities provided by quantum electronic phenomena. Here the transport may well be more ballistic in nature rather than statistical as described by current transport approaches. This scale has certain very real advantages over present day device scales, since some limiting processes such as dielectric breakdown (impact ionization) will be largely eliminated, although interband tunneling will probably be present but at much higher field strengths.

In approaching the question, we have introduced the archetypal MSD as a MOS device of channel length 2500Å and discussed the relevant spatial and temporal scales that are important for transport within this structure [18] We have examined the important time, distance, velocity, and energy scales that are important in small semiconductor devices. For this medium-small device, we find that we are already approaching the time and distance scales that raise serious objections to usage of a semi-classical approach to transport theory within the device. As a consequence, major modifications are required to both the collision interactions in the Boltzmann transport equation, due to intra-collisional field effects arising from a breakdown of the independent perturbation approximation, and to the current response equations within the device. In this last case, effects arise not only due to spatial and temporal relaxation of the carriers and charge density, but

also due to retardation effects within the current response. The MSD thus represents not only the logical lower limit expected from scaling arguments, but also the lower limit for which performance can be expected to follow extrapolations from current experience. Even here, though, we expect major modifications in the detailed response functions for the device. As a result, frequency and power limitations in small devices can be expected to be significantly different from predicted values based upon extrapolations from large devices. Let us now consider the VSD.

Although it has been demonstrated that lithography is capable of fabricating linewidths and spacings of 250Å, this is not a sufficient condition for actually fabricating a device. However, we have demonstrated how such a device, a p-channel MESFET, can in fact actually be fabricated from current technology, utilizing two side processing of the semiconductor wafer, here assumed to be silicon [19]. However, it was pointed out that already in the MSD, the limits of applicability of the Boltzmann transport equation (BTE) were reached. This implies that for the VSD, transport must be considered from a fully quantum mechanical viewpoint. The foundation for this was laid by establishing that a distribution function picture is still valid. We have carried this forward utilizing the full density matrix for the carriers, phonons, and environment. We showed that a BTE-like equation results, although the specific meaning of the effective distribution function is obviously different. The role of the environment is especially important, since in many cases it can provide a renormalization of the energy scales such as in size-quantization of superlattices. In the MSD, it was shown that a displaced Maxwellian distribution function was appropriate [18,20]. For the VSD, we have shown that since a BTE-like transport equation is obtained, moment equations can be developed, as in the MSD, using an analgous

formulation to the displaced Maxwellian, i.e.-a "displaced" density matrix form of the distribution function.

If one can summarize the difficulties that arise in these small devices, the primary problem is the very fast time scales inherent in small devices. See, for example, Fig. 1, where we plot the appropriate scales that one can encounter in small devices. An electron travelling at 10^7 cm/sec can cross 0.1 micron length in 10^{-12} sec. On this time scale, the electrons encountering a high-field region of this dimension, such as the pinch-off region in a MOSFET, do not have adequate time to establish any sort of equilibrium distribution, a point made rather pointedly earlier by Ruch [21], and by Maloney and Frey [22]. Additional complications arise from the fact that the collision duration is no longer negligible on this time scale and strongly affects the transport dynamics [23,24,25].

In the following sections, we examine the consequences of changes that the short-time scales play on the transport of carriers in these small devices. First, we look at the effect of the non-negligible collision duration and the concommitant intra-collisional field effects. Then we turn to its effect on the transport equations, especially with regard to transient dynamic response. In this latter regard, the concept of diffusion on this time scale must be carefully examined.

A. The Intra-Collisional Field Effect (ICFE)

The Boltzmann transport equation (BTE) has long been the basis for semi-classical transport studies in semiconductors and other materials. Its utility also stems from the fact that is is readily transformable into a path-variable form which can be adapted to numerical solutions for complicated energy-dependent scattering processes [26,27]. In this form, the

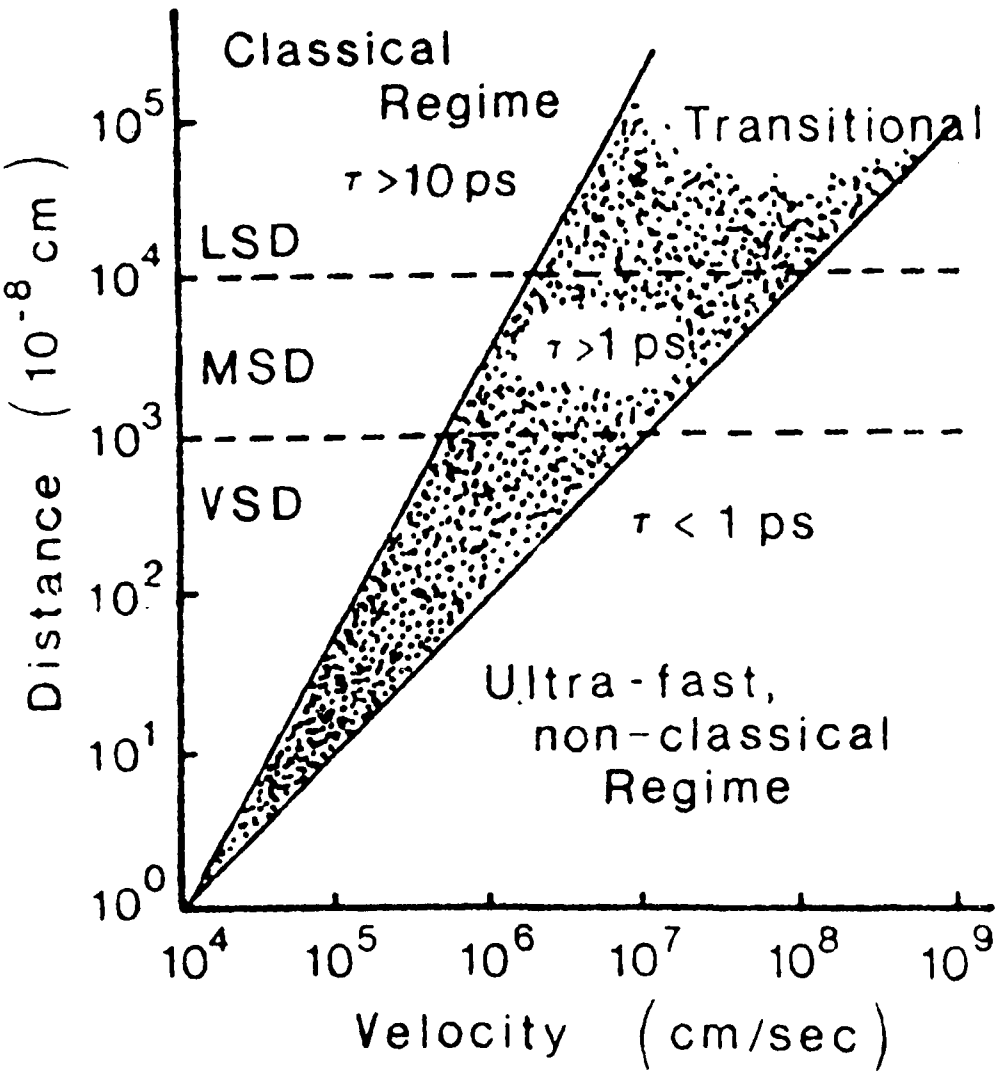

Fig. 1. Temporal and spatial variables for small semiconductor devices.

BTE is often referred to as the Chambers-Rees path integral equation, and serves as the basis for Monte Carlo and iterative calculation of transport. However, the BTE is valid only in the weak coupling limit under the assumptions that the electric field is weak and slowly varying at most, the collisions are independent, and the collisions occur instantaneously in space and time. Each of these approximations can be expected to be violated in future sub-micron dimensioned semiconductor devices. We have shown that in such devices, the time scales are such that collision durations are no longer negligible when compared to the relevant time scale upon which transport through the device occurs [18,19]. In this situation, even for time-independent fields, the quantum kinetic equations are nonlocal in time and momentum. It may be recalled that the BTE can be rigorously derived from the density matrix Liouville equation formulation of quantum transport [24,28]. In the BTE approach, the collision terms are derived under the assumption that the collisions occur instantaneously, which is a reasonable approximation when the mean-time between collisions is large. At high fields, such as will occur in very small devices, the collision duration is significant and correction terms must be generated (for the BTE) to account for the non-zero time duration of each collision. If the instantaneous collision approximation that leads to the BTE is relaxed, an additional field contribution appears as a differential super-operator term (see, e.g., the discussion in ref. 18) in the collision integrals evaluated in the momentum representation, resulting in an intra-collisional field effect [24,25].

The intra-collisional field effect (ICFE) can be partially understood by referring to Fig. 2. In the Boltzmann case, the collision occurs instantaneously, so that the carrier enters the collision sphere at a and exits at b. However, the collision does not occur instantaneously, but

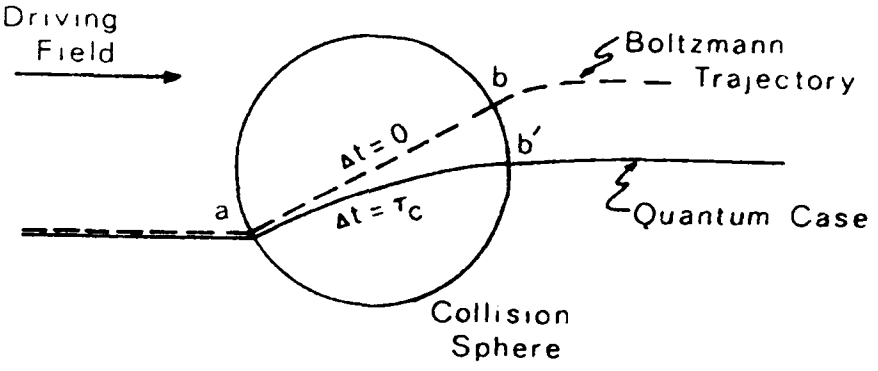

Fig. 2. Naive picture of a collision event. The intra-collisional field effect modifies the trajectory through the collision thus affecting the collision dynamics.

requires a non-zero collision duration τ_c. In this case, it can now be accelerated by the field *during the collision*. Thus it exits not at b, but at b' some time $\Delta t = \tau_c$ later. When τ_c begins to become comparable to τ, the mean time between collision, this ICFE will have a significant effect on the transport dynamics, particularly in the transient response region.

The mathematical details of the ICFE have previously been given [24], so we shall not go into these details here. Rather, we shall give some of the supportive evidence for the observability of the effect. In very large fields, such as can occur in SiO_2 near breakdown, the ICFE can indeed be very significant [29]. Two major modifications of the scattering integral occur as a result of this intra-collisional process. First, the total energy-conserving δ-function is broadened by the presence of the electric field. Second, the threshold energy required for the emission of an optical phonon is modified, which causes a shift (in energy) of the δ-function. This latter process is easily understood in physical terms. The argument of the energy conserving δ-function is just

$$E_f - E_i \pm \hbar\omega_o = E(\vec{p}_f) - E(\vec{p}_i) \pm \hbar\omega_o \tag{1}$$

but the initial and final momenta evolve during the collision as

$$\vec{p}(t') = \vec{p} - \int_{t'}^{t} e\vec{E}(t'')dt'' \quad , \tag{2a}$$

$$\vec{p}'(t') = \vec{p}' - \int_{t'}^{t} e\vec{E}(t'')dt'' \quad . \tag{2b}$$

In the emission of an optical phonon, where the electron is scattered against the electric field, the field will absorb a portion of the electron's energy during the collision, and hence a reduction in energy loss to the

lattice will be favored. The opposite effect, an enhancement in energy loss to the lattice, occurs for emission along the electric field. These effects can be incorporated into the appropriate scattering integrals in the iterative technique, and this has been carried out [29]. For electric fields above (5-6) x 10^6 V/cm, the broadening and shift of the scattering resonances produce a noticeable effect upon the velocity-field relationship and a reduction in threshold can be observed in the calculated impact ionization rates in SiO_2. In fig. 3, we show these rates as measured by Solomon and Klein [30] and as calculated earlier [29]. It is necessary to include effects arising from the ICFE to adequately fit theory to experiment. The second major effect of the ICFE arises for scattering between non-equivalent sets of valleys [31]. There, the ICFE causes a virtual lowering of the final state valleys with respect to the initial state valleys. However, this effect is not large in realistic devices.

Although the ICFE is exceedingly large in SiO_2 because of the polar nature of the phonons here, it is also significant in the case of Si. In fig. 4, we plot the collision duration versus field and compare it with the momentum relaxation time $\tilde{\tau} = m^*\mu e$, where $\mu = v_d/F$ is the mobility. The effect this has on the velocity-field curve is shown in Fig. 5. Also shown is the countering effect of collision retardation discussed in the next section. The ICFE is especially noticeable at high fields, where it essentially eliminates the scattering by the low energy intervalley phonon [32]. This phonon is already weakly coupled since scatters through a first-order interaction [33] but is normally an effective scatterer at high fields.

B. The Retarded Transport Equations

When the ICFE is included as a modification of the lowest order kinetic equations, a high field quantum kinetic equation, which replaces the BTE,

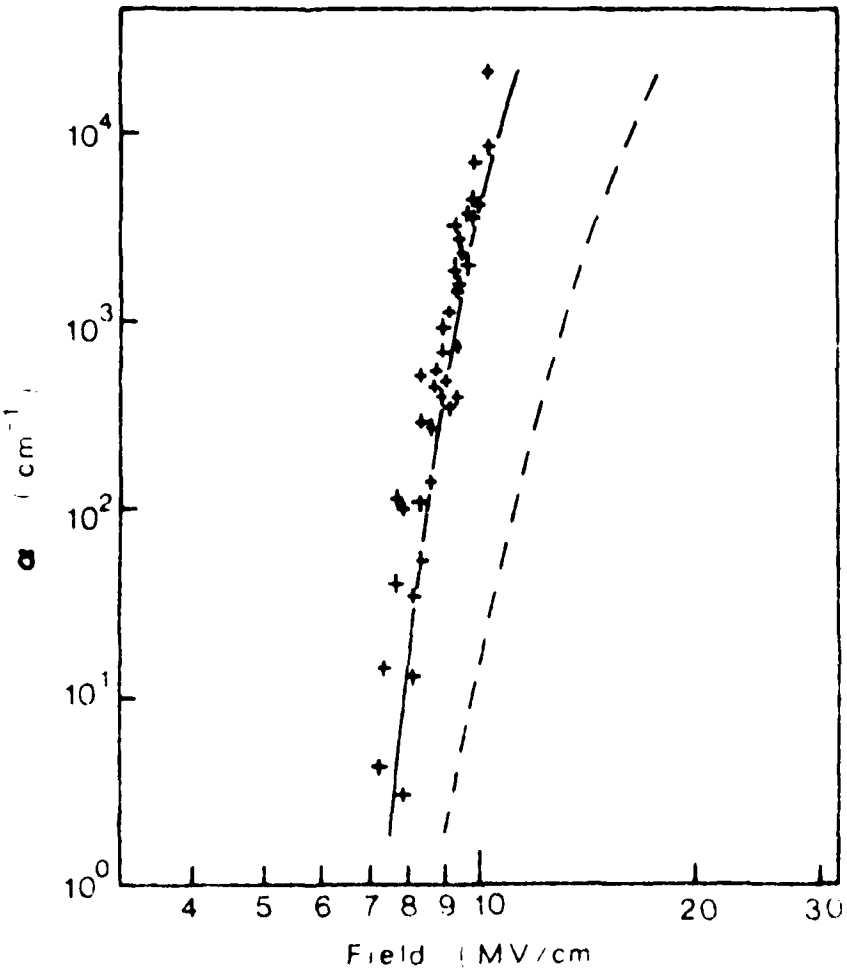

Fig. 3. Ionization rates in SiO_2 as a function of field. The dashed curve is for $m_h/m_e = 100$ and ignores the subthreshold phonon emission. The solid curve takes into account subthreshold emission, for $m_h \sim 2.9m_o$. Data is due to Solomon and Klein [17]. This is fairly substantive evidence for the presence of the ICFE.

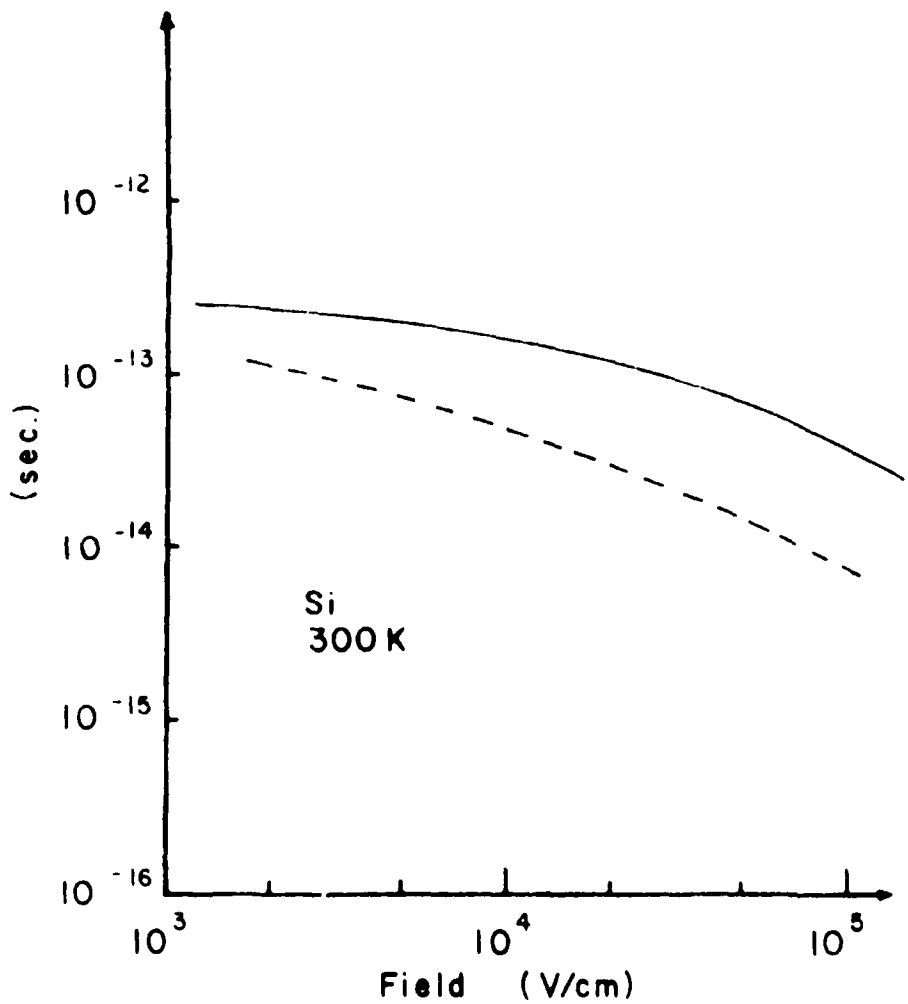

Fig. 4. Variation of the effective collision duration (dashed curve) and mean-free time for Si (solid curve). The latter quantity is calculated from the effective mobility as $\bar{\tau} = m^*\mu/e$.

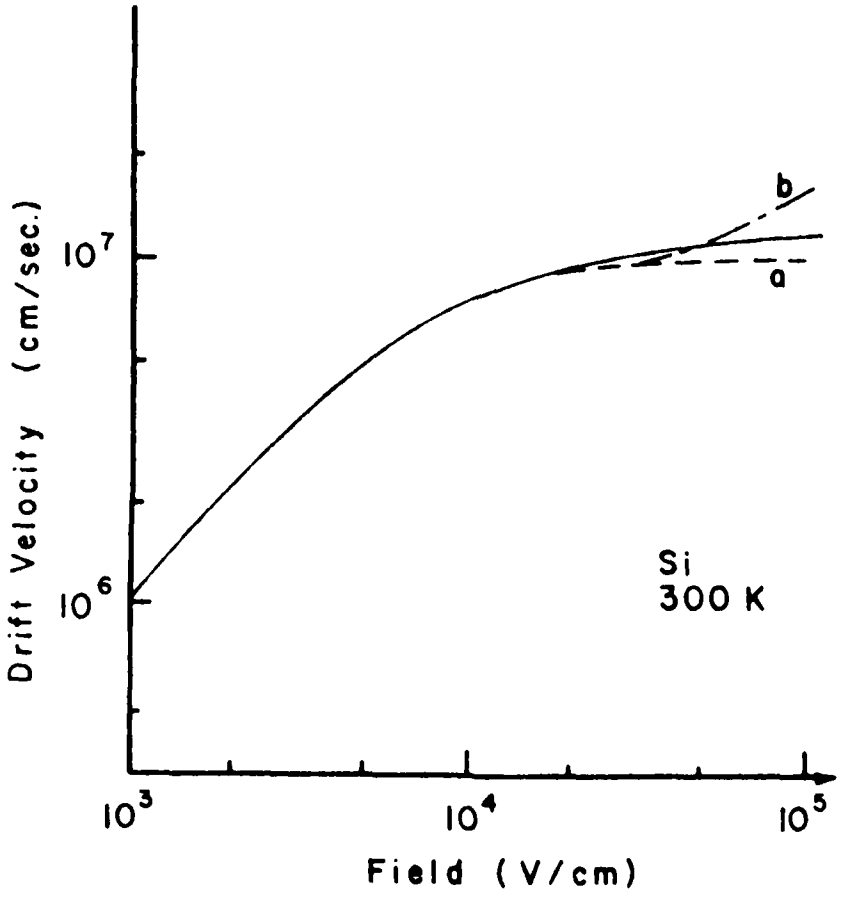

Fig. 5. The velocity-field curve for electrons in Si as calculated by a drifted Maxwellian approach. At high fields, the field weakens the collisions (dot-dashed curve, b) causing an increase of velocity although the collisional retardation stops this effect (solid curve). The low-frequency curve normally encountered is the dashed curve, a.

is found as [24,34]

$$\frac{\partial f(\vec{p},t)}{\partial t} + e\vec{E}(t) \cdot \nabla_p f(\vec{p},t) = \int_0^t dt' \sum_{\vec{p}'} \{S(\vec{p},\vec{p}';t,t') f(\vec{p}',t') - S(\vec{p}',\vec{p};t,t') f(\vec{p},t')\} \quad , \tag{3}$$

where the momenta $\vec{p},\vec{p}'$ are explicit functions of the retarded time t' on the right-hand-side through the relationship of Eq. (2), and the transition terms S take the form, for inelastic phonon scattering,

$$S(p,p';t,t') = \mathrm{Re}\,\frac{2\pi}{\hbar} \sum_{\vec{q}} \left(\frac{1}{\pi\hbar}\right) \exp\left(-\frac{t-t'}{\tau_\Gamma}\right) x \tag{4}$$

$$x\,(N_q + \tfrac{1}{2} + \tfrac{1}{2}\eta)\,|V(q)|^2\,\delta_{\vec{p},\vec{p}'} + \eta_{\vec{q}} \exp\left[-i \int_t^{t'} \frac{dt''}{\hbar}\,\beta(\vec{p},\vec{p}';t'')\right] \quad ,$$

where β is the argument of the normal δ-function and is given by Eq. (1). The two exponential factors in (4) are related to the joint spectral density function, which reduces to an energy conserving δ-function in the instantaneous collision, low-field limit, $\varepsilon(\vec{p})$ is the quasi-particle renormalized energy, $\hbar/\tau_\Gamma$ is the joint linewidth due to collisional broadening of the initial and final states, and η takes the values +1, -1 for phonon emission or absorption, respectively, in the in-scattering term. For the out-scattering term, the role of $\vec{p}$, $\vec{p}'$ are interchanged, although this does not upset detailed balance in the equilibrium sense.

In small semiconductor devices, where the dimensional scale is of the order of 1.0 μm or less, the carrier concentration will in general be relatively high [8]. Fröhlich [35] first pointed out that the isotropic part of the carrier distribution function is Maxwellian provided that the carrier concentration exceeds a certain critical concentration; i.e.--provided that the rate of inter-carrier energy exchange was sufficiently large. Under these conditions, the anisotropic terms in the distribution function are small and

a parameterized distribution function, often called the displaced Maxwellian, can be utilized [36]. With this assumption, a hierarchy of moment equations can be generated from the BTE, from which the various parameters can be determined (see, e.g., the discussion in [23,24]). In this work, we extend these moment equations to include first-order effects arising from the non-zero time duration of the collision. Under the conditions prescribed above for the drifted Maxwellian distribution function, the most general nondegenerate distribution which will be stationary under the presence of collisions is of the form [37]

$$f(E) = \exp[-\beta_e(E - \vec{v}_d \cdot \vec{p})] \quad , \tag{5}$$

where β_e and v_d are functions of time and $\beta_e = 1/k_B T_e$. However, this form is instantaneous in time, and we need rather a proper retarded function. Such a function is suggested by the expansion of (5) as

$$f(E) \simeq \exp(-\beta_e E)[1 + \vec{v}_d \cdot \vec{p}\beta_e] \tag{5a}$$

and a recognition of the form required for the memory functional [34]. To achieve this form, we specify f(E) by the ansatz [this form is not unique, but it is not felt at present that the results are critically dependent on the form assumed]:

$$f(E) = \int_0^t d\tau[\delta(t - \tau) - \vec{v}_d (t - \tau) \cdot \frac{d}{d\tau} (\vec{p} \frac{d}{dE})] f_o (E,\tau) \quad , \tag{5b}$$

where the two derivatives are required, respectively, to preserve the dimensionality and to bring β_e into the second expression in the bracket. In the limit of long times (5b) reduces to (5a). Here, $f_o = \exp(-\beta_e E)$.

Starting from the density-matrix developed form of the BTE, we have shown previously that collision terms derived in the normal case, but modified

for intra-collisional field effects must be convolved with a decay effect over an effective collision duration [23]. Thus, the balance equations are modified in a straightforward fashion, although the details are much more complicated. This latter follows from the role of the intra-collisional field effects, which both broaden and shift the resonances, effectively lengthening the effective collision duration and weakening the effect of the collision itself. If (3) is Laplace Transformed, the moment equations can be developed by multiplying by an arbitrary function $\phi(\vec{p})$, integrating over the momentum with (5b), so that the moment equations are developed in the transform-domain, and then retransforming [38]. This yields the energy-balance equation

$$\frac{\partial}{\partial t}\left(\frac{3}{2} k_B T_e\right) = e\vec{F} \cdot \vec{v}_d(t) - \frac{1}{\bar{\tau}_c} \int_0^t \exp(-\tau/\bar{\tau}_c) \langle \Gamma_E(t - \tau) \rangle d\tau \qquad (6)$$

where we have recognized that $\langle \phi \rangle = 3k_B T_e/2$ when $\phi = E$. In addition, the momentum balance equation is

$$m^* \frac{\partial v_d}{\partial t} = eF - \frac{m^*}{\bar{\tau}_c} \int_0^t v_d(t - \tau) \int_0^\tau \langle \Gamma_m(\tau - \tau') \rangle e^{-\tau'/\bar{\tau}_c} d\tau' d\tau \quad . \qquad (7)$$

If $\tau_c \to 0$ and v_d is slowly varying, then (7) reduces to the normal

$$m^* \frac{\partial v_d}{\partial t} = eF - m^* v_f \Gamma_m \quad , \qquad (8)$$

and Γ_m is recognized as the rate of momentum relaxation ($= 1/\tau_m$). The various convolutions introduce a significant temporal retardation in the rate of momentum relaxation.

C. Application to Silicon

Calculations have been carried out to ascertain the effect of the collisional retardation in a number of semiconductors [20,38]. Here we treat only silicon. The parameters used for Si were the normal values:

$m_\ell = 0.91m_o$ and $m_t = 0.19m_o$. Intervalley scattering was treated by two effective phonons [32], a 630 K zero-order coupled phonon and a 190 K first-order coupled [33] phonon. Coupling constants of 9×10^8 eV/cm and 5.6 eV, respectively, were taken for these two modes, as they give a good description not only of the low field mobility as a function of temperature, but also to the high-field velocity in quasi-two-dimensional inversion layers [39]. These values differ somewhat from recent iterative [40] and Monte Carlo [41] calculations, but these latter treatments should be interpreted carefully as they use an improper treatment of the low-energy phonons.

In fig. 6 is shown the transient reponse of the electrons to a steady homogeneous field of 20 kV/cm. Although the τ_c retardation acts to speed up the response, the dominant factor is the memory effect of $\dot{r}_m$ and v_d. The collisional retardation speeds up the process, however, primarily due to the effect of slowing down changes in the effective energy via collisional relaxation.

D. The Semiconductor Device Model

In order to evaluate the role of the above transport effects on actual device performance, we have developed a two-dimensional simulation of a MESFET. We have used a submicron structure, with 0.25 μm source-drain spacing, to put us under the scaling limit. In this manner, the device performance is dominated by the carrier transport dynamics. An exact two-dimensional numerical analysis of a submicron n-InAs Cold-FET was performed [42]. The model used a finite difference approach and an algorithm developed to solve the coupled set of differential equations. The program solved Poisson's equation using a FFT technique [43,44].

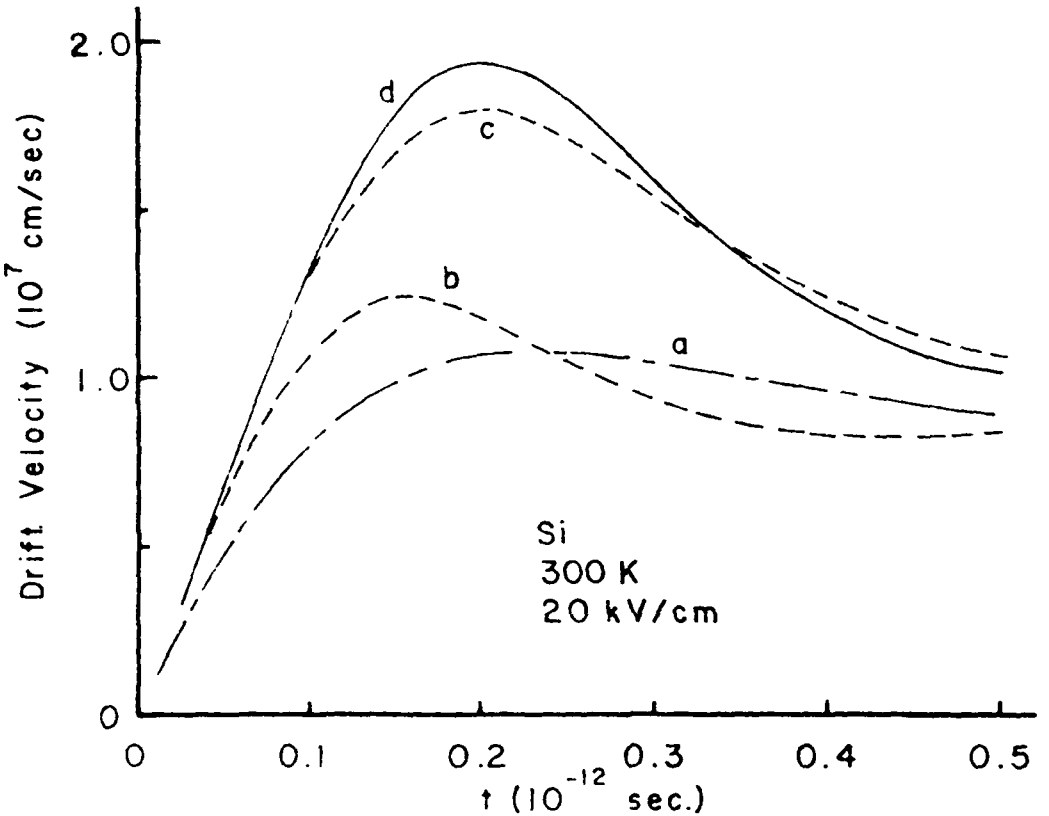

Fig. 6. Transient dynamic response of carriers in silicon. It is assumed the carriers see a homogeneous field of 20 kV/cm that is applied at t = 0. Curve a shows the response neglecting the short-time effects, but including the weakening of the collision in the high-field. Curve b includes the effects of retardation due to the non-zero collision duration alone, curve c includes the memory effects alone, and curve d includes all effects according to Eq. (7) of the text.

The electric field and current density were updated from the solution of Poisson's equation and the continuity equation then solved to update the charge concentration using a fourth-order predictor-corrector integration routine [45]. The currents are obtained at the drain, gate and source, and a test on the overall consistency is made; a negative outcome starts the process over again, while a positive outcome accepts the results.

An n-channel device with parallel source and drain contacts to eliminate geometrical effects due to co-planar placement was used. The bulk of the FET consisted of an n-InAs epitaxial channel layer on top of an n^- substrate. All calculations were performed assuming a channel doping of $5 \times 10^{17} cm^{-3}$ and a substrate doping of $1 \times 10^{13} cm^{-3}$. The drift current in the channel was obtained using a field dependent mobility curve obtained previously for InAs at 77 K [45]. The device channel dimension was 0.25 μm and the active depth 0.04 μm. The gate length was 0.065 μm. All calculations were normalized to the width of the device, taken to be 1.0 μm. Neumann boundary conditions were applied to all insulating surfaces in the device and Dirichlet boundary conditions to all the contacts. Ohmic contacts were simulated on the source and drain by forcing charge neutrality.

InAs does not readily form Schottky barriers with many materials [47]. This absence of a barrier in n-type material, with even highly electronegative metals such as gold, has been confirmed by measurements in the ternary system InGaAs [48]. Thus the metal used and the doping concentration under the gate must be carefully considered. Schottky barriers on covalent compound semiconductors have been suggested as being a function of the anion electronegativity [49], and this suggests a candidate metallization. A material that may show some merit in producing a Schottky

barrier in InAs is $(SN)_x$ [50]. $(SN)_x$ has an electronegativity about 0.1 eV higher than gold, and hence should be able to produce a Schottky barrier with a barrier height of about 0.025 eV, adequate for the device suggested here. Even lacking such a Schottky barrier, a barrier can be induced by a blocking contact produced by a doping notch [51]. Because of the uncertainty in the actual barrier height, the calculated characteristics are referenced to an effective gate bias $V'_g = \phi_b - V_g$.

In fig. 7, we show the I-V curves obtained from the 2-D numerical simulation of the submicron InAs Cold-FET. Although a highly saturated drain current is not obtained, good FET behavior is illustrated. In fig. 8, we show the charge density within the device.

The transconductance g_m can be extracted from the I-V curves, and the value of g_m obtained at V_d = 0.1 V is approximately 800 millimhos. The maximum gate capacitance is obtained by assuming a fully depleted condition. The value of C_g was estimated to be 2×10^{-16} f. From these values of g_m and C_g, an RC switching time-constant can be evaluated as C_g/g_m which is 2.5×10^{-14} sec. However, the transient response is routinely calculated in the program, and a switching time of 7.8×10^{-14} sec was obtained. This value is longer than that obtained from g_m and C_g above, and can be explained if the gate-to-drain parasitic capacitance dominates the switching characteristics. These values lead to a power-delay product $P\text{-}t_d$ on the order of 10^{-18} joules, easily competitive with the best estimates for Josephson-junction logic gates.

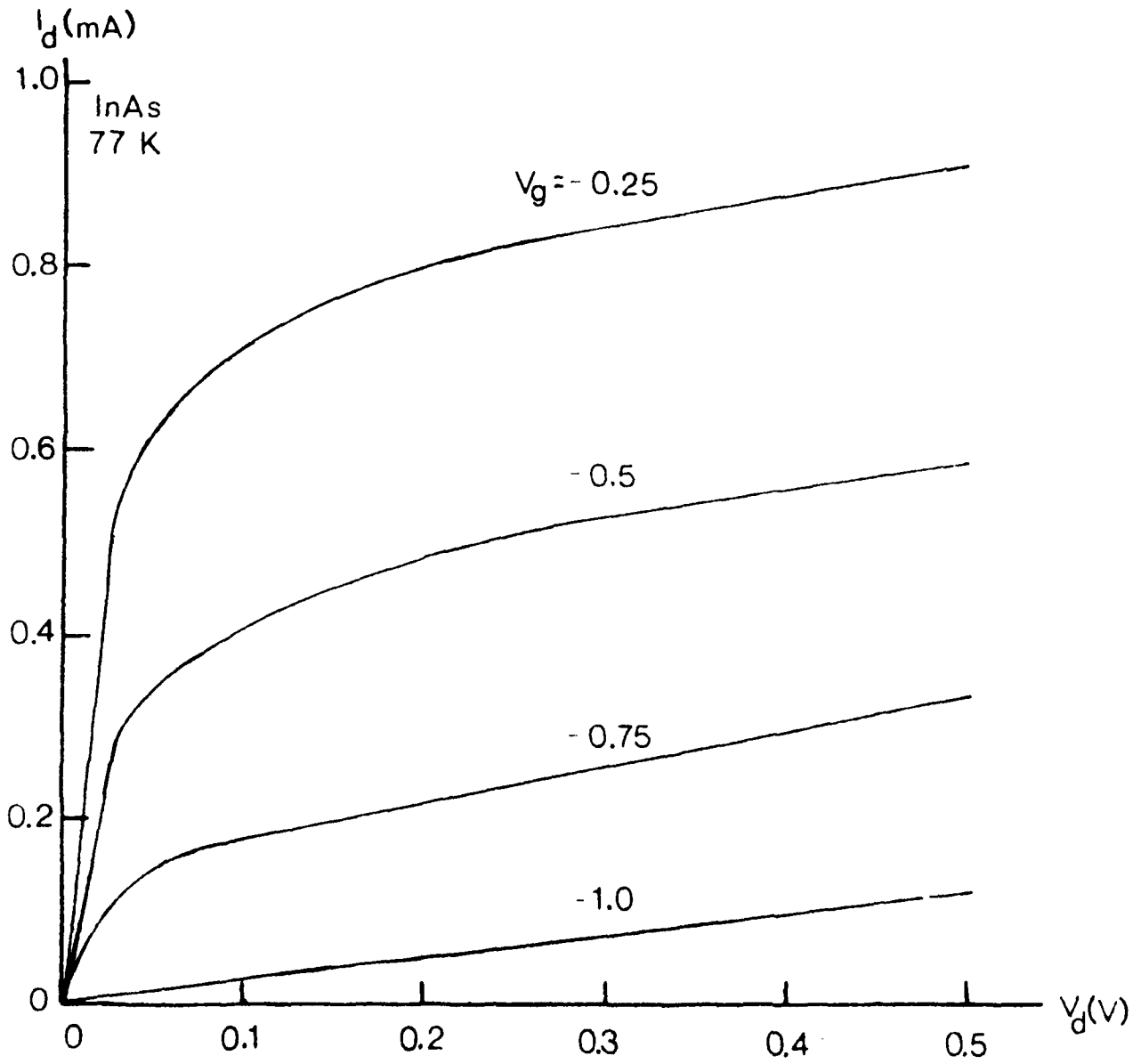

Fig. 7. Output characteristics for the InAs FET. The reduced gate voltage, V'_g, is the sum of the built-in potential, ϕ_b, and the applied gate bias, as discussed in the text.

Fig. 8. Charge concentration plot looking directly down on the gate contact. The charge concentration increases in the vertical direction and is normalized to the active channel doping. The length of the plot corresponds to the length of the FET device and the direction into the plot is the depth of the device.

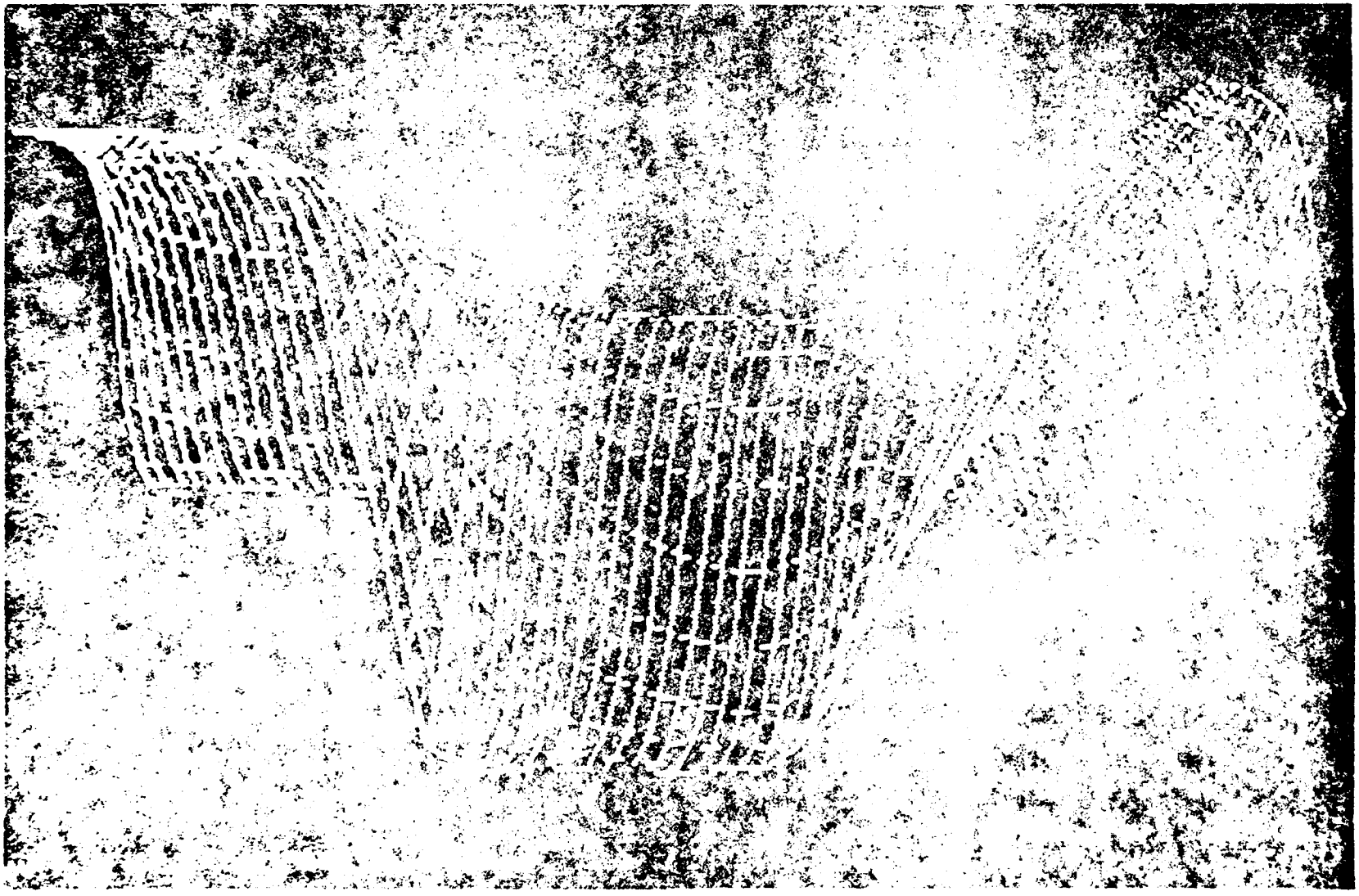

III. References

1. G. Moore, Proc. Intern. Electron Device Mtg., 1975 (IEEE Press, 1975) p. 11
2. This conclusion is usually drawn from the fact that the latest 32k and 64k memory chips were introduced at such a date that they fall below the extrapolation of Ref. 1. It is not clear that these represent sufficient data points to draw such a conclusion.
3. V. L. Rideout, F. H. Gaensslen, and G. LeBlanc, IBM J. Res. Develop. 19, 50 (1975). This and the following four references are meant to be representative of current technology and no attempt will be made to give an exhaustive list of references on such technology.
4. T. J. Rogers, R. Hiltpold, J. W. Zimmer, G. Marr, and J. D. Trotter, IEEE J. Sol. State Circuits SC-11, 614 (1976).
5. M. J. DeClerq and T. Laurent, IEEE J. Sol. State Circuits SC-12, 264 (1977).
6. J. M. Herman and S. A. Evans, IEEE J. Sol. State Circuits SC-12, 93 (1977).
7. R. C. Eden, B. M. Welch, and R. Zucca, IEEE J. Sol. State Circuits SC-13, 419 (1978).
8. B. Hoeneisen and C. A. Mead, Sol.-State Electr. 15, 819 (1972).
9. B. Hoeneisen and C. A. Mead, Sol.-State Electr. 15, 891 (1972).
10. For a recent review, see R. W. Keyes, Science 195, 1230 (1977), and references contained therein.
11. I. E. Sutherland, C. A. Mead, and T. Everheart, Basic Limitations in Microcircuit Fabrication Technology, Report R-1956-ARPA (Rand Corporation, 1976). This same conclusion was reached in discussion

sessions at the recent Conference on Hot Electrons in Semiconductors, Denton 1977. See, e.g., D. K. Ferry, Sol.-State Electr. 21 319 (1978).

12. A. N. Broers, J. M. E. Harper, and W. W. Molzen, Appl. Phys. Letters 33, 392 (1978).
13. A. N. Broers, W. Molzen, J. Cuomo, and N. Wittels, Appl. Phys. Letters 29, 596 (1976).
14. M. T. Elliott, M. R. Splinter, A. B. Jones, and J. P. Reeskin, IEEE Trans. Electron Dev. ED-26, 469 (1979).
15. This result was reported by R. Reynolds of DARPA during a recent electronics review.
16. F. Fang, private communication.
17. In fact, a good introduction to some of these effects, as they are found in GaAs, can be found in H. Kroemer, Sol.-State Electr. 21 61 (1978), and in H. Grubin, in Nonlinear Electron Transport in Semiconductors, Ed. by D. K. Ferry, J. R. Barker, and C. Jacoboni (Plenum, New York, 1980) p. 311. These are seminal review papers and should be required reading for serious device physicists.
18. J. R. Barker and D. K. Ferry, Sol.-State Electr. 23, in press (1980), App. A.
19. D. K. Ferry and J. R. Barker, Sol.-State Electr. 23, in press (1980), App. B.
20. D. K. Ferry and J. R. Barker, Sol.-State Electr. 23, in press (1980).
21. J. G. Ruch, IEEE Trans. Electron Dev. ED-19, 652 (1972).
22. T. J. Maloney and J. Frey, J. Appl. Phys. 48, 781 (1977).
23. D. K. Ferry and J. R. Barker, Sol.-State Commun. 30, 361 (1979).
24. J. R. Barker, J. Phys. C 6, 2663 (1973); Sol.-State Electr. 21, 267 (1978).

25. K. K. Thornber, Sol.-State Electr. 21, 259 (1978).

26. P. J. Price, Sol.-State Electr. 21, 9 (1978).

27. D. K. Ferry, in Handbook of Semiconductors, Vol. 1., Ed. by W. Paul (North-Holland, Amsterdam, in press).

28. W. Kohn and J. M. Luttinger, Phys. Rev. 108 , 590 (1957).

29. D. K. Ferry, J. Appl. Phys. 50, 1422 (1979).

30. P. Solomon and N. Klein, Sol. State Commun. 17, 1397 (1975).

31. J. R. Barker, Physics Letters, in press.

32. For a discussion of scattering in Si, see e.g., D. L. Long, Phys. Rev. 120, 2024 (1960).

33. D. K. Ferry, Phys. Rev. B 14, 1605 (1976).

34. Actually, this is a special case, in its generic form, of a transport equation arising from the generalized Master Equation. See, e.g., R. Zwanzig, J. Chem. Phys. 40, 2527 (1964); Phys. Rev. 124, 983 (1961); M. S. Green, J. Chem. Phys. 20, 1281 (1952); 22, 398 (1954); R. Kubo, J. Phys. Soc. Jpn. 12, 570 (1957); H. Mori, Phys. Rev. 112, 1829 (1958).

35. H. Fröhlich , Proc. Roy. Soc. A188, 521 (1947).

36. H. Fröhlich and B. V. Paranjape , Proc. Phys. Soc. (London) B69, 21 (1956); R. Stratton , Proc. Roy. Soc. A242, 355 (1957); A246, 406 (1958).

37. R. Peierls , in Lecture Notes in Physics 31: Transport Phenomena Ed. by J. Ehlers, K. Hepp and H. A. Weidenmüller , (Springer-Verlag, Berlin, 1974) p. 2.

38. D. K. Ferry and J. R. Barker, J. Phys. Chem. Sol., in press.

39. D. K. Ferry, Phys. Rev. B 14, 5364 (1976).

40. J. G. Nash and J. W. Holm-Kennedy, Appl. Phys. Letters 27, 38 (1975).

41. C. Jacoboni, C. Canali, G. Ottaviani and A. Alberigi-Quaranta, Sol.-State Electron. 20, 77 (1977).

42. R. K. Reich and D. K. Ferry, IEEE Trans. Electron Dev., in press.

43. J. P. Christianson and R. W. Hockney, Comp. Phys. Comm. 2, 127 (1971).

44. S. P. Yu and W. Tantraporn, in 6th Biennial Cornell Conf. on Active Microwave Devices (1977), p. 399.

45. R. W. Hamming, Numerical Methods for Scientists and Engineers, McGraw-Hill, New York (1962).

46. R. C. Curby and D. K. Ferry, Phys. Rev. B 3, 3379 (1971).

47. S. L. Kurtin, T. C. McGill, and C. A. Mead, Phys. Rev. B 3, 3368 (1971).

48. K. Kajiyama, Y. Mizushima, and S. Sakata, Appl. Phys. Letters 23, 458 (1973).

49. J. O. McCaldin, T. C. McGill, and C. A. Mead, J. Vac. Sci. Tech. 13, 802 (1976).

50. R. A. Scranton, J. S. Best, and J. O. McCaldin, J. Vac. Sci. Tech. 14, 930 (1977).

51. H. Kroemer, IEEE Trans. Electron Dev. ED-15, 819 (1968).

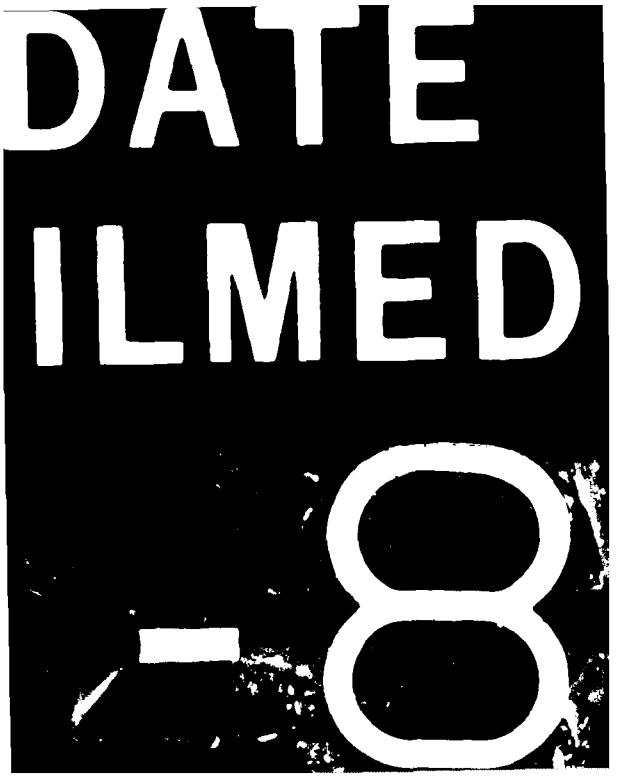
DATE
ILMED
-8